JOURNAL OF GEOPHYSICAL RESEARCH, VOL. 91, NO. A4, PAGES 4543–4550, APRIL 1, 1986

Jovian VLF Chorus and Io Torus Aurora

U. S. INAN

STAR Laboratory, Stanford University, Stanford, California

A test particle model of the cyclotron resonance interaction of waves and trapped radiation belt particles is used to estimate the energetic electron fluxes precipitated by Jovian VLF chorus waves observed on the Voyager 1 and 2 spacecraft near the Io torus. The precipitation fluxes induced by 1-s-long chorus wave packets at $L \simeq 7.6$ and 8.6 are estimated to be bursts of $\sim$ 5s duration with a peak of 0.3–3 and 0.7–7 ergs/cm^2 s that consist of electrons of $\sim$5–100 keV energy and that arrives at the ionosphere $\sim$ 15 s after the generation of the chorus wave at the equatorial plane. The effects in the Jovian ionosphere of the chorus-induced precipitation are estimated using existing ionospheric models. A possible experiment for measuring Jovian chorus-induced aurora is proposed and discussed.

1. INTRODUCTION

Many types of plasma waves were observed by the Voyager 1 and 2 spacecraft in the Jovian magnetosphere; among these, VLF chorus emissions have attracted considerable attention [*Scarf et al.*, 1979*a*; 1981]. A comparative analysis of terrestrial and Jovian chorus revealed many similarities in the measured parameters but important differences in the theoretical parameters that are relevant to the generation mechanisms of these emissions [*Inan et al.*, 1983]. A detailed discussion of the observed spectral features of chorus and possible mechanisms that may account for them was presented by *Coroniti et al.* [1984].

The pitch angle diffusion of energetic particles by whistler mode waves in the Jovian magnetosphere near the Io plasma torus was discussed by a number of authors [*Fillius et al.*, 1976; *Scarf et al.*, 1979*b*]. Specifically, it was estimated that the chorus waves observed at $L \simeq 8$ may precipitate fluxes of a few ergs cm^{-2} s^{-1} consisting of electrons in the few keV range [*Coroniti et al.*, 1980]. This earlier estimate was based on linear diffusion coefficients and stable trapping limits applied to equatorial interactions. In this paper we utilize a test particle model of the wave-particle interaction, including the computation of the full nonlinear trajectories of the near-resonant particles and accounting for interactions that occur away from the equator as the chorus waves propagate along the field lines after being generated near the equator. This method allows us to estimate the dynamic energy spectra of the chorus-induced precipitation that would be incident on the Jovian ionosphere, including the time variation of the energy flux and the energy of the electrons that constitute the flux. While our model provides new predictions of the energy-time features, our results are in general agreement with the initial estimate of the peak flux levels reported by *Coroniti et al.* [1980]. Using the computed dynamic spectra of the precipitating electrons and a model of the Jovian ionosphere, we also present a first order estimate of the secondary ionization that would be created by the incident electron flux at 500-1000 km ionospheric altitudes.

The estimated chorus-induced energetic electron fluxes of a few ergs/cm^2 s led to suggestions [*Coroniti et al.*, 1979] that this effect may make a significant contribution to the observed Io torus aurora [*Sandel et al.*, 1979]. However, recent work has shown that the role of such electrons in the Jovian aurora is uncertain. Considerations based on the total estimated power in the Jovian aurora and various possible contributing waves and wave-particle interaction mechanisms indicate that >500 keV precipitating ions may be a more likely factor [*Thorne*, 1983]. On the other hand, the scattering mechanism for ions cannot be established, and the available experimental data are not sufficient to rule out the contribution of chorus-induced electron precipitaton.

The characteristic features of chorus-induced aurora as estimated here can aid in the planning of experiments designed for testing the hypothesized association of VLF chorus and the Io torus aurora. One such experiment is briefly discussed. This concept involves (1) the detection of ionospheric perturbations resulting from the chorus-induced particle precipitation with the aid of a radio beacon signal that is occulted by the Jovian ionosphere, and (2) the measurement of Jovian chorus waves using a plasma wave receiver. Although simultaneous measurement of the two effects may be difficult to achieve in the near future, the measurements of the chorus waves and ionospheric effects can be separately carried out in the upcoming Galileo mission, and radio beacon data from auroral occultations can be compared with chorus data on a statistical basis.

2. DESCRIPTION OF THE MODEL

The test particle model that is used here was originally developed for and applied to cyclotron resonant interactions between whistler mode waves and energetic particles in the terrestrial magnetosphere [*Inan et al.*, 1982]. Recent extensions of this model have included interactions between relativistic particles and waves with slowly varying frequency [*Chang and Inan*, 1983*a*; *Chang et al.*, 1983]. The latter is particularly important since both terrestrial and Jovian VLF chorus emissions generally exhibit such frequency variations [*Burtis and Helliwell*, 1976; *Coroniti et al.*, 1984].

Comparisons of the theoretical model with experimental observations of wave-induced particle precipitation effects in the earth's magnetosphere have produced generally satisfactory results [*Chang and Inan*, 1983*b*; *Carpenter et al.*, 1984]. In one case, involving direct satellite-based observations of electrons precipitated by man-made waves, the application of the model to the data has led to improved understand-

Paper number 5A8832.
0148-0227/86/005A-8832$02.00

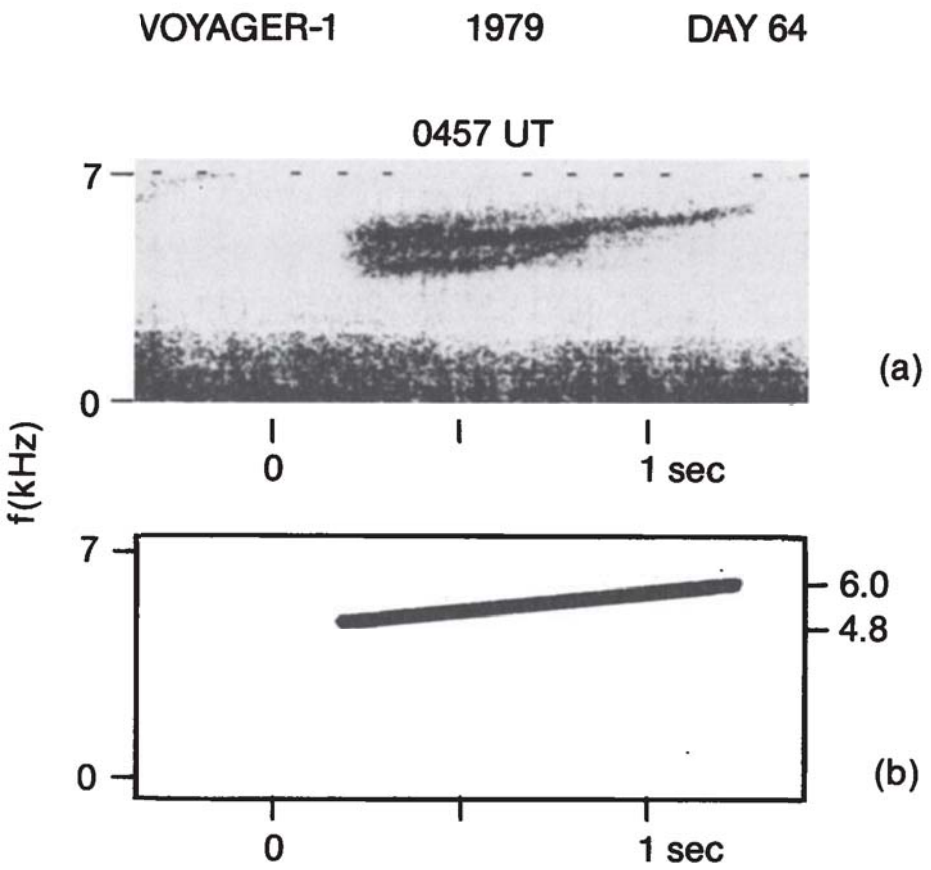

Fig. 1. (*a*) A discrete Jovian VLF chorus element observed on Voyager 1 (taken from *Inan et al.* [1983]). (*b*) The frequency-time spectrum of the chorus wave pulse used in the test particle model.

ing of the dynamics of the near loss cone particles and to the "calibration" of the theoretical model [*Inan et al.*, 1985]. As a result, the test particle model can be more confidently applied to make predictions and to help in the planning of future experiments [*Chang and Inan*, 1985]. It is in this spirit that we undertake the application of the model to the case of Jovian VLF chorus.

The approach used in the test particle simulation is based on computing the nonlinear trajectories of a large number of near-resonant test particles and using these to infer the wave-induced perturbations of the trapped particle distribution function and the resulting precipitated flux [*Inan et al.*, 1978]. The resonant encounters of the wave with particles (distributed over varying ranges of energy and local pitch angle) as the wave packet propagates along the field line are taken into account. The contributions to the precipitated flux from interactions at different points along the field line are integrated, considering the travel times of the wave and the particles to and from the interaction regions [*Inan et al.*, 1982]. The result is usually presented as the precipitated energy flux as a function of time that would be observed at the ionosphere and the energies of the particles that constitute the flux at different times during the wave-induced precipitation burst.

Cold Plasma Model

We assume field-aligned wave propagation with $\mathbf{k} \| \mathbf{B}_0$, where $\mathbf{k}$ is the wave vector and $\mathbf{B}_0$ is the static magnetic field, which is assumed to be that of a centered dipole. The variation of the cold plasma density along the magnetic field lines is assumed to be given by

$$N_e(z) = N_{e_0} \exp\left[-\left(\frac{z}{H}\right)^2\right] \qquad (1)$$

where z is the distance from the centrifugal equator along the magnetic field lines and H is the scale height. For the wave-particle interaction considered here the variation of electron density is the dominant factor in determining the interaction length [*Inan et al.*, 1983]. Thus, in the following, "equator" refers to the centrifugal rather than the magnetic equator.

Modeling based on cold plasma measurements and whistler dispersion has been consistent with a range of values for the scale height of $H \simeq 1$–$2R_J$, with $R_J \simeq 71,323$ km being the radius of Jupiter [*Bagenal and Sullivan*, 1981; *Gurnett et al.*, 1981]. In our model calculations we use $H \simeq 1.5R_J$. Based on Voyager 1 measurements, the radial variation of the equatorial density was taken to vary as $L^{-7.4}$ [*Bagenal and Sullivan*, 1981; *Birmingham et al.*, 1981; *Gurnett et al.*, 1981] with the plasma density at $L \simeq 8$ at the equator being $N_{e_0} \simeq 230$ cm^{-3} [*Bagenal et al.*, 1980].

To assure that whistler mode propagation of the chorus can occur along the field line outside the torus, a constant electron density of 1 cm^{-3} was added to the electron density obtained from (1). A similar correction was previously used to interpret the dispersion of whistlers observed on Voyager

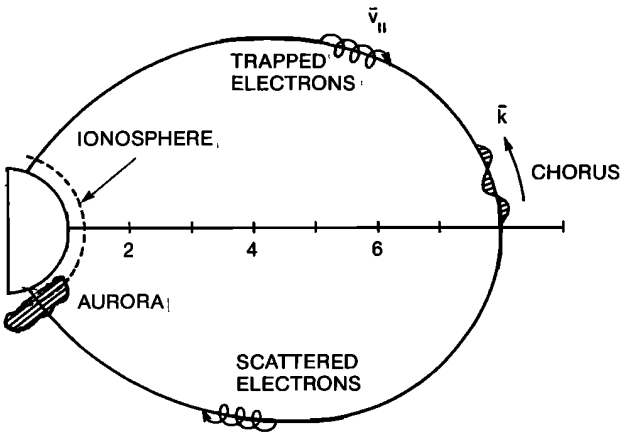

Fig. 2. Schematic description of the chorus-induced precipitation phenomenon. The chorus wave pulse is assumed to be spontaneously generated near the equator. As it propagates along the field lines away from the equatorial region, it interacts in the gyroresonance mode with counterstreaming particles of increasing energy. The pitch angle scattered particles are precipitated in the opposite hemisphere.

1; such a lower limit to the electron density at all points along a field-aligned propagation path is consistent with the observed upper cutoff frequency of whistlers [*Gurnett et al.*, 1981].

Trapped Particle Distribution

We assume the energetic particle distribution near the Io torus to be proportional to E^{-n}, where E is the particle energy. The differential energy spectrum for 1-keV particles at 90° pitch angle was taken to be 10^{10} el cm^{-2} s^{-1} sr^{-1} keV^{-1} [*Scudder et al.*, 1981]. The pitch angle distribution is "isotropic" except for a sharp loss cone, which for $L = 8$ is $\sim 1.8°$. Note, however, that the chorus-induced precipitation is primarily due to particles that are within a few degrees of the loss cone. Therefore, our assumption of an isotropic distribution is only important to the extent that it determines the flux level at the edge of the loss cone for a given flux at 90° pitch angle. This is further discussed in the next section.

Using reported data from Voyager 1 measurements of few keV particles [*Scudder et al.*, 1981] and higher energy electrons [*Krimigis et al.*, 1979] we estimate the energy dependence parameter n to be in the range $n \simeq 2$–3. For the model calculations below, we use a value of $n = 3$.

3. Chorus-Induced Aurora

Wave Characteristics

We consider an isolated chorus element that is generated at time $t = 0$ at the equator at $L \simeq 8.6$, where the cold plasma density is taken to be $\sim$135 cm^{-3} (see previous section). An example of such an element observed on Voyager 1 is shown in Figure 1*a* [*Inan et al.*, 1983]. For use in our model, we represent this wave packet with a coherent signal of 1-s duration having a linear frequency variation over the range 4.8–6.0 kHz, as shown in Figure 1*b*. The wave intensity at the equatorial plane for 6 kHz was taken to be $B_w = 10$ pT, consistent with magnetic field values inferred from the wave electric fields measured on Voyager 1 [*Coroniti et al.*, 1980].

In an earlier study of the gyroresonant wave-particle interaction parameters in the Jovian magnetosphere, we have demonstrated that a 10-pT field intensity is larger than the threshold field intensity for phase trapping of particles in the wave's potential well [*Inan et al.*, 1983]. While this is true for particles having pitch angles of $\alpha \simeq 45°$, we note that the precipitation fluxes discussed below consist only of electrons that are within a few degrees of the equatorial loss cone ($\sim$1.8°). Since the wave-trapping force is proportional to $B_w \tan\alpha$ [*Inan et al.*, 1978], the trajectories of the near loss cone particles are for the most part quasi-linear, with phase trapping of the particles not being a significant factor. Note that the absence of significant phase trapping also implies that our representation of the diffuse chorus burst with a quasi-monochromatic wave as shown in Figure 1 is a reasonable approximation.

We note here that while our analysis is aimed at estimating the precipitation flux due to a single chorus element, our result can be directly used to estimate the fluxes due to a sequence of chorus elements or other single chorus elements observed on slightly different L shells. This point is discussed further below.

Interaction Geometry and Resonant Particle Energy

The spontaneously generated chorus wave is assumed to propagate away from the equator along the magnetic field

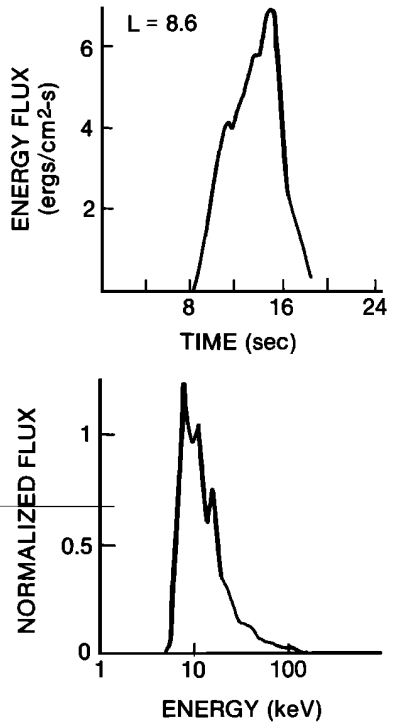

Fig. 3. (*a*) The precipitated energy flux induced by the Jovian VLF chorus element shown in Figure 1 propagating at $L \simeq 8.6$, where the equatorial cold plasma density is $N_e \simeq 135$ cm^{-3}. The flux is that which would be observed at 1000 km altitude in the hemisphere opposite from the one toward which the chorus pulse propagates. The time $t = 0$ refers to the time of spontaneous chorus generation near the equator. (*b*) The time-integrated energy spectrum showing the relative contribution to the energy flux of particles of different energies.

lines. In doing so, it interacts in the cyclotron resonance mode with counterstreaming electrons as depicted in Figure 2. The electrons are pitch angle scattered as a result of this interaction and a fraction of the particle population is precipitated out of the trapped orbits. As shown in Figure 2, the precipitation flux would be incident on the Jovian ionosphere at the opposite end of the field line.

As it propagates away from the equator, the whistler mode wave interacts with electrons of different energies in accordance with the cyclotron resonance condition

$$f + \frac{k}{2\pi} v_{\parallel} \simeq f_H \qquad (2)$$

where f and f_H are the wave frequency and electron gyrofrequency, respectively, $v_{\parallel}$ is the particle parallel velocity, and k is the wave number, which for longitudinal propagation is given by $k \simeq (18\pi\sqrt{N_e}/c)\sqrt{f/(f_H - f)}$ with c being the speed of light.

For a centered dipole model as considered here, the gyrofrequency increases with distance from the equator, while the electron density decreases in accordance with (1). For the Jovian magnetosphere near $L \simeq 8$ the dominant variation is dN_e/dz, since the gyrofrequency variation over a typical interaction length is negligible [*Inan et al.*, 1983]. Thus the resonant particle energy ($\propto v_{\parallel}^2$) as obtained from (2) varies as N_e^{-1} and therefore increases with z.

Model Results: Dynamic Spectra of Chorus-Induced Aurora

With the various parameters specified as discussed above, the test particle model can be used to estimate the time evolution of the chorus-induced aurora. Results of the model calculation are shown in Figures 3 and 4. Figure 3a shows the precipitated energy flux as a function of time, with $t = 0$ representing the time at which the chorus element originated at the equatorial plane. The flux is seen to consist of a burst of ~5 s duration (full width half maximum), with the peak flux arriving at the ~ 1000 km altitude at $t \simeq 15$ s. The magnitude of the peak flux is ~7 ergs cm^{-2} s^{-1}, although this depends on the trapped flux level near the loss cone as discussed below.

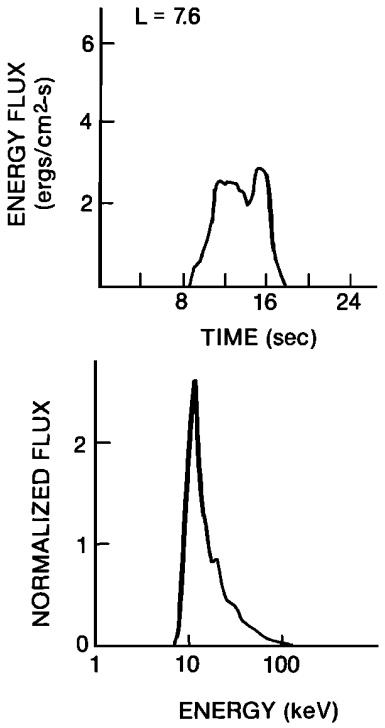

Fig. 4. Dynamic spectrum of Jovian chorus-induced aurora for the $L = 8.6$ case shown in Figure 3. The top and bottom panels show the same diagram seen from two different perspectives.

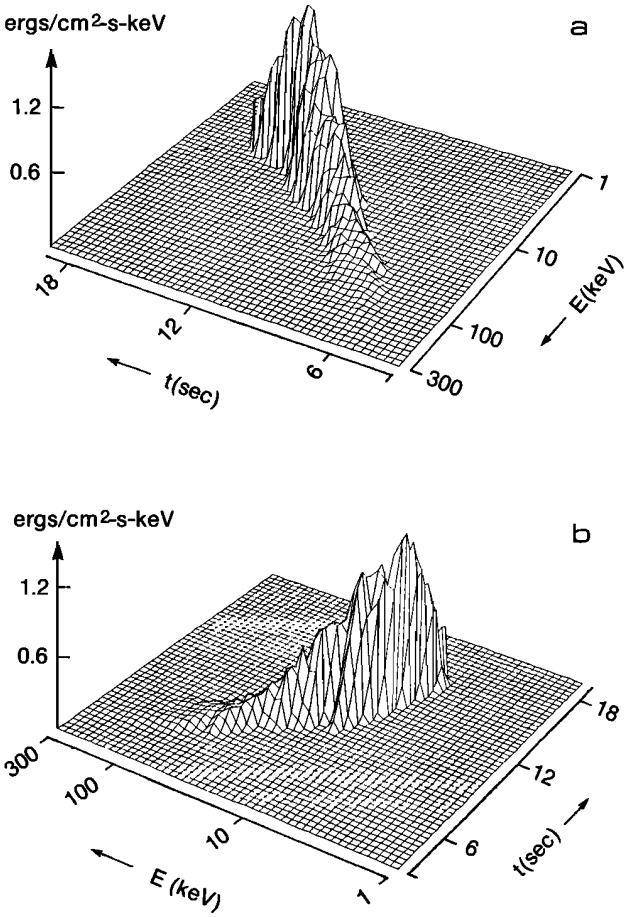

Fig. 5. (*a*) The precipitated energy flux induced by a single Jovian chorus element of 1-s duration with linearly increasing frequency in the 8.5–9.5 kHz range, generated at $t = 0$ the equator at $L \simeq 7.6$ where the cold plasma density is $N_e \simeq 336$ cm^{-3}. (*b*) The time-integrated energy spectrum showing the relative contribution to the energy flux of particles of different energies.

Figure 3b shows the time-integrated energy spectrum of the precipitation burst. The flux consists of particles in the 5–100 keV energy range, with most of the contribution coming from particles with ≤ 20 keV energy.

The dynamic spectrum of the same chorus-induced precipitation burst is shown in Figure 4. The top and bottom panels show two different perspectives of the same three-dimensional flux-energy-time diagram. We see that the higher-energy particles arrive at the ionosphere earlier, in spite of the fact that they encounter the chorus wave farther away from the equator than the lower-energy particles. However, the energy flux is higher for the lower-energy particles which interact with the wave closer to the equatorial plane and thus suffer more pitch angle scattering [*Inan et al.*, 1978]. This is also due to the fact that the trapped particle distribution function was assumed to fall off with energy, being proportional to E^{-3}

The characteristic energy-time signature of the chorus-induced precipitation burst is determined by a combination of factors, including the wave and particle travel times, the energy and latitude dependence of the gyroresonant pitch angle scattering, and the assumed energetic particle distribution. The result shown in Figure 4 is similar to the dynamic spectra of wave-induced precipitation bursts predicted for the earth's magnetosphere [*Chang and Inan*, 1985]. The much longer length of the Jovian field lines is the main reason for the much larger delay (~15 s) between the generation of chorus element and the arrival of the flux at the ionosphere.

Discussion

We have estimated the characteristics of the electron precipitation flux that would be induced by a single isolated chorus element of the kind shown in Figure 1. This element was chosen because of its relatively well-defined spectral content. The Voyager 1 observations at ~ 0457 UT represent only a small fraction of Jovian chorus observations. An extended period of chorus activity was also observed later (up to 0600 UT) as the spacecraft moved toward the planet into the L shell range $7 < L < 8$ [*Coroniti et al.*, 1984; *Inan et al.*, 1983]. However, as was shown by *Inan et al.* [1983], much of the characteristics of the observed chorus (in terms of the wave field intensity, normalized wave frequency (f/f_{Heq}) spectral shape) did not change significantly between 0457 and 0600 UT. The variation of various wave-particle interaction parameters (such as resonant particle energy, wave-particle interaction length, threshold field intensity) as a function of L shell and normalized wave frequency were investigated by *Inan et al.* [1983]. According to these results, and for given normalized wave frequency, the equatorial resonant particle energy does not change appreciably between $L = 9$ and $L = 7$, and the interaction length at $L = 7$ is only ~25% lower than that at $L = 9$. This indicates that the precipitation pulses computed for the chorus burst of Figure 1 should be representative of precipitation induced by other observed single elements of Jovian chorus.

To illustrate this further, we have used the test particle model to compute the precipitation flux induced by another single chorus element observed at $L \simeq 7.6$. This element was modeled by a 1-s long pulse having 10 pT intensity and linearly increasing frequency between 8.5 and 9.5 kHz. The cold plasma density was taken to be ~366 cm^{-3}. The results of the model computation are shown in Figure 5. We see that the temporal signature is very similar to the $L \simeq 8.6$ case, except for the fact that the peak flux is somewhat lower. The energy range of the particles constituting the flux is ~8–100 keV.

Most terrestrial magnetospheric chorus as well as Jovian VLF chorus observed by Voyager 1 and 2 consists of bands of emissions made up of successive, sometimes overlapping discrete elements such as that in Figure 1 [*Scarf et al.*, 1981]. The associated precipitation in such a case can be expected to be a superposition of successive precipitation pulses of the kind presented in Figures 3 and 4, since wave-induced pitch angle scattering by a single wave pulse typically depletes a very small percentage of the available flux near the loss cone [*Inan et al.*, 1985]. While this situation would change some minutes after the onset of the chorus band, the near loss cone flux might remain high due to scattering of particles at even higher pitch angles. Such aspects of the problem are beyond the scope of this paper and must be addressed in the context of a self-consistent model that includes the source functions and drift of the particles across flux tubes, as well as the effect of the modified particle distribution on the chorus generation.

While the fact that chorus emissions are excited indicates that the pitch angle distribution is anisotropic, the scattering of electrons by the wave packet may not necessarily occur near the generation region. Furthermore, the chorus-induced precipitation is primarily due to particles that are within a few degrees of the loss cone, whereas the particles that are responsible for the generation and amplification of chorus may be at higher pitch angles. Observational evidence on the pitch angle distribution of energetic electrons in the Io torus is not available. However, for an anisotropic distribution, the near loss cone flux, and therefore the chorus-induced precipitated flux, would typically be lower than the estimates given above. For example, if one assumes a pitch angle distribution proportional to $(0.2 \sin^{0.2} \alpha + 0.8 \sin^{12} \alpha)$, one that has been used to describe highly anisotropic distributions in the earth's magnetosphere [*Anderson*, 1976], the ratio of the 90° flux to that near the loss cone would be a factor of ~10. In view of this, the peak flux for the computed chorus-induced precipitaton bursts of Figures 3 and 5 is taken to be 0.3–3 and 0.7–7 ergs/cm^2 s, respectively.

The peak flux computed with the test particle model is of the same order of magnitude as the value (~6 ergs cm^{-2} s^{-1}) estimated by *Coroniti et al.* [1980]. This is interesting since the two estimates are based on quite different methods. We note that *Coroniti et al.* [1980] only considered equatorial interactions and used a strong diffusion assumption and quasi-linear theory for evaluating the diffusion coefficients. Since the chorus frequency range at $L \simeq 8$ was taken to be 8.5–9.5 kHz, the flux estimated consisted of particles of few keV energy. In our case, we consider the specific chorus element shown in Figure 1 covering the frequency range of 4.8–6.0 kHz and observed at $L \simeq 8.6$, as well as another element covering the frequency range of 8.5–9.5 kHz observed at $\simeq 7.6$. Since we also account for off-equatorial interactions, the chorus-induced aurora is found to consist of particles in the 5–100 keV energy range.

In the next section we discuss the effects on the Jovian ionosphere of a precipitation pulse such as the one shown in Figure 4.

4. Ionospheric Effects of Chorus-Induced Aurora

The aeronomical effects of energetic particle precipitation into the Jovian atmosphere were recently discussed by *Waite et al.* [1983]. Using a theoretical model, *Waite et al.* considered the precipitation of 1-and 10-keV electrons at auroral as well as mid-latitudes. Estimates of the background ionospheric electron density profiles and secondary ion production rates were presented for the altitude ranges of 300–1500 km. In the following, we use these results to obtain a first-order estimate of the ionospheric effects of chorus-induced aurora.

The background ionospheric electron density (in the absence of precipitation) at ~500 km altitude is estimated to be ~2×10^4 cm^{-3} and is mainly due to solar extreme ultraviolet radiation (EUV). The ion production rate due to

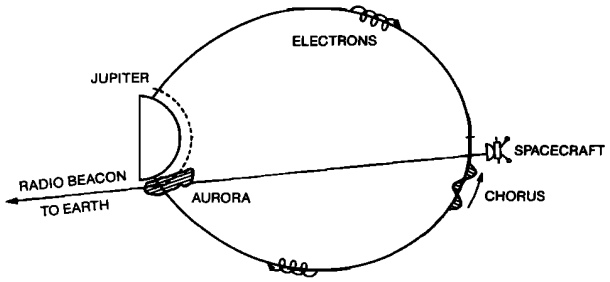

Figure 6. Schematic description of a possible experiment to measure the association between Jovian VLF chorus and the aurora. The chorus waves are observed at the equatorial plane with a plasma wave receiver on board the satellite. The radio beacon signal is occulted by the Jovian ionosphere and can in principle be used to detect ionospheric density enhancements resulting from secondary ionization due to the chorus-induced precipitation bursts. While the simultaneous measurement of chorus and the ionosphere may not be possible due to orbital constraints, data from radio occultations of the auroral ionosphere can be compared with chorus data acquired at other times.

an incident flux of $\sim$10 ergs cm^{-2} s^{-1} of 10-keV electrons reaches a maximum at $\sim$500 km altitude. This maximum is $\sim 2\times 10^4$ cm^{-3} s^{-1} or $\sim 2\times 10^3$ cm^{-3} s^{-1} for the production of H_2^+ or H^+, respectively [*Waite et al.*, 1983]. Since H_2^+ production accounts for a much larger proportion of the energy deposition [*Waite et al.*, 1983] and since the production rate is higher, we consider H_2^+ as the main secondary ionization component.

Assuming the chorus-induced auroral burst to consist of $\sim$10 keV particles and to last for $\sim$5 s, the secondary ionization at $\sim$500 km altitude would be $\sim 10^5$ el/cm^3. This consitutes an increase above the background EUV-associated density of a factor of $\sim$5. On the other hand, at $\sim$ 600 km altitude where the background density is estimated to peak at $\sim 10^6$ el/cm^3, [*Waite et al.*, 1983], the aurora-induced enhancement would still be $\sim 10^5$ el/cm^3, constituting only $\sim$10% of the background. However, we also note here that the Voyager 2 radio science experiment measurements indicate that the peak value for the background density may not be higher than $\sim 2\times 10^5$ el/cm^3, in which case the chorus-induced perturbation would be of order $\sim$50% [*Eshleman et al.*, 1979a].

5. A Proposed Experiment for Detecting Chorus-Induced Aurora

We found above that the auroral fluxes expected to be induced by Jovian VLF chorus can give rise to significant secondary ionization in the Jovian ionosphere at 500–600 km altitudes. This finding raises the intriguing question of whether these transient ionospheric signatures can be measured in association with chorus. We propose one such measurement, involving the observation of chorus waves on a planetary probe near the equator at L =4–10 in the Io torus and the detection of temporal changes in the ionosphere via a radio beacon signal from the same satellite that is occulted by the Jovian ionosphere along its propagation path to the earth. The concept of such an experiment is depicted in Figure 6.

Radio occultation experiments have proved to be powerful tools for exploring the vertical structure and small-scale dynamics of planetary atmospheres and ionospheres (for the case of Jupiter, see *Eshleman et al.* [1977, 1979*a*, *b*], *Lindal et al.* [1981], and *Hinson and Tyler* [1982]). In general, these techniques are applied under the assumption that the properties of the region under observation do not change appreciably with time during the experiment. Time variations in the signals received from the occulted spacecraft are attributed to the rapid transverse motion of the propagation path across a spatially varying field of refractive index.

For application of radio techniques to detect transient effects such as chorus-induced aurora and the associated density enhancements, the reverse must be assumed; it must be postulated that spatial changes over the time scales concerned are negligible. The time scale of interest here is the duration of the precipitation burst which from Figure 4 is $\sim$5s. For a spacecraft velocity of $\sim$10 km/s near the magnetic equator, the change in altitude of the occulted region would be $\sim$50 km for the worst case geometry. If the orbital track of the spacecraft is approximately along the line-of-sight path to the earth, the change in altitude can be much smaller. Thus the proposed measurement must rely on the assumption that the vertical ionospheric density profile does not vary over an $\sim$50 km range. This may be a good assumption for $\sim$600 km but probably is not as good for $\sim$500 km, since the latter is very near the bottom edge of the Jovian ionosphere where the density varies roughly exponentially with altitude [*Waite et al.*, 1983]. However, the background density variation with altitude would be expected to vary in a predictable manner, so that it might still be possible to look for temporal fluctutations on top of a varying background. In any case, when precipitation of 10-keV particles does occur, they are deposited in a broad height range centered at $\sim$500 km altitude, so that the variation of the secondary ionization over a 50-km range can be assumed to be negligible for a first-order calculation.

The detectability of chorus-induced aurora using radio techniques depends on the percentage density change $\delta N/N$ as well as the spatial distribution of the irregularities. For example, *Hinson and Tyler* [1982] have observed scattering of radio waves from ionospheric irregularities in the size range of 1–100 km, corresponding to a $\delta N/N \simeq$ 5–10%. In that case, the ionosphere was assumed to have an irregular, corrugated structure that appeared to be statistically homogeneous over an altitude interval of several thousand kilometers. In contrast, the precipitation-induced ionospheric perturbation may occur in a single more localized region. In such a case the phase and amplitude perturbations of the coherent radio beacon would be fundamentally different.

While no information exists on the size or distribution of the precipitation region(s) due to a single chorus element, in the following we conservatively assume a region of $\sim$100 km in horizontal extent and covering a height range of 50–100 km. The spatial extent of chorus waves and/or associated precipitation regions is not well known even in the terrestrial magnetosphere; however, existing evidence from multistation ground-based and simultaneous satellite-ground observations indicates that the regions may be at least as large as a few hundred kilometers in extent [*Carpenter et al.*, 1985; *Smith et al.*, 1985].

For a single localized precipitation region of $\sim$100 km latitudinal extent and for the geometry depicted in Figure 6, the detectability of the perturbation can be assessed by computing the percentage change in the total electron content along the signal path. For an exponential background ionosphere

and a peak density of $\sim 10^5$ el/cm^3, the total electron content on an occultation path having a minimum altitude of ~500 km would be $\sim 10^{14}$ cm^{-2} [*Hinson*, 1983]. Assuming aurora-induced density enhancement of $\sim 10^5$ el/cm^3 deposited uniformly over a path of ~100 km horizontal extent, the differential change in the total electron content would be $\sim 10^{12}$ cm^{-2}. Based on previously reported measurements from Voyager 1 and 2, such differential changes in total electron electron can be detected. For example, *Eshleman et al.* [1979*a*, *b*] have reported background ionospheric measurements of electron concentration as low as $\sim 10^3$ el/cm^3, which would correspond to a total electron content along the path of $\sim 10^{12}$ cm^{-2} [*Hinson*, 1983].

Discussion

Based on the above first-order analysis, we conclude that the ionospheric density enhancements caused by chorus-induced aurora can be detected using the radio occultation technique. Thus, the experiment depicted in Figure 6 can in principle be used to simultaneously observe such effects and the chorus waves, if the indicated orbit geometry can be achieved. An orbit configuration as shown did not occur during the Voyager 1 and 2 encounters of Jupiter. However, radio beacon data from the occultations of the auroral regions were acquired, and these data can be analyzed for signatures of chorus-induced precipitation, in the light of expected characteristics as estimated in this paper. The results can then be compared with chorus observations near the equator, acquired at other times but nevertheless on the same field lines connecting to the auroral regions.

An upcoming opportunity for carrying out such an experiment would have been the Galileo mission that will be launched during 1986 and that includes a satellite to be placed in orbit around Jupiter. However, an examination of the planned orbital configuration indicates that occultation of the auroral regions would not occur during times when the satellite would be near the equatorial plane on L shells of L=4–10. In view of this, opportunities for carrying out the simultaneous measurement of chorus and auroral effects are not likely to be available. On the other hand, some opportunities would undoubtedly exist for carrying out measurements of the auroral regions using radio beacon occultation techniques. Such data can then be searched for signatures of chorus-induced precipitaton in the light of the predictions put forward in this paper and compared on a statistical basis with chorus data obtained at other times but on similar field lines.

6. Summary and Conclusions

We have estimated the dynamic energy spectrum of the electron precipitation flux that would be induced via gyroresonance interactions of trapped radiation belt electrons and Jovian VLF chorus waves. The precipitation burst induced by 1-s long chorus wave packets generated near the magnetic equator at $L \simeq 8.6$ and 7.6 was estimated to consist of particles having energy ~5-100 keV. The energy flux consists of bursts of ~5 s duration with a peak of ~0.7–7 ergs cm^{-2} s^{-1} at $L \simeq 8.6$ (0.3–3 ergs cm^{-2} s^{-1} at $L \simeq 7.6$) that arrive at the ~1000 km ionospheric altitude ~15 s after the generation of the chorus emission at the equatorial plane.

The chorus-induced precipitation burst is expected to produce density enhancements of order $\sim 10^4$–10^5 cm^{-3} at 500-600 km altitudes in the Jovian ionosphere. Such transient perturbations of the Jovian ionosphere are detectable using radio beacon techniques. A new experiment is thus proposed, aimed at simultaneously measuring Jovian VLF chorus waves and the ionospheric effects of precipitation induced by the chorus. While the proposed simultaneous measurement requires a very specific orbital configuration that does not seem likely for the upcoming Galileo mission, data from radio beacon occultations of the auroral regions can be used to search for signatures of chorus-induced precipitation that can then be compared with chorus data acquired at other times.

Acknowledgments. I acknowledge discussions with colleagues in the STAR Laboratory. The contributions of D. Hinson on the general concepts of the proposed experiment as well as to the text of section 4 were especially useful and are greatly appreciated. The figures and the text were prepared by P. Pecen and K. Fletcher. This research was supported by the National Aeronautics and Space Administration under grant NAGW-653.

The Editor thanks D. A. Gurnett and F. Scarf for their assistance in evaluating this paper.

References

Anderson, R. R., Wave particle interactions in the evening magnetosphere during geomagnetically distrubed periods, Ph.D. thesis, Univ. of Iowa, Iowa City, 1976.

Bagenal, F., and J. D. Sullivan, Direct plasma measurement in the Io torus and inner magnetosphere of Jupiter, *J. Geophys. Res., 86,* 8447, 1981.

Bagenal, F., J. D. Sullivan, and G. L. Siscoe, Spatial distribution of plasma in the Io torus, *Geophys. Res. Lett., 7,* 41, 1980.

Birmingham, T. J., J. K. Alexander, M. D. Desch, R. F. Hubard, and B. M. Peterson, Observations of electron gyroharmonic waves and the structure of the Io torus, *J. Geophys. Res., 86,* 8497, 1981.

Burtis, W. J., and R. A. Helliwell, Magnetospheric chorus: Occurrence patterns and ormalized frequency, *Planet. Space Sci., 24,* 1007, 1976.

Carpenter, D. L., M. L. Trimpi, R. A. Helliwell, and J. P. Katsufrakis, Perturbations of subionospheric LF and MF signals due to whistler-induced electron precipitation bursts, *J. Geophys. Res., 89,* 9857, 1984.

Carpenter, D. L., U. S. Inan, E. W. Paschal, and A. J. Smith, A new VLF method for studying burst precipitation near the plasmapause, *J. Geophys. Res., 90,* 4383, 1985.

Chang, H. C., and U. S. Inan, Quasi-relativistic electron precipitation due to interactions with coherent VLF waves in the magnetosphere, *J. Geophys. Res., 88,* 318, 1983*a*.

Chang, H. C., and U. S. Inan, A theoretical model study of observed correlations between whistler mode waves and energetic electron precipitation events in the magnetosphere, *J. Geophys. Res., 88,* 10053, 1983*b*.

Chang, H. C., and U. S. Inan, Lightning-induced electron precipitation from the magnetosphere, *J. Geophys. Res., 90,* 1531, 1985.

Chang, H. C., U. S. Inan, and T. F. Bell, Energetic electron precipitation due to gyroresonant interactions in the magnetosphere involving coherent VLF waves with slowly varing frequency, *J. Geophys. Res., 88,* 7037, 1983.

Coroniti, F. V., F. L. Scarf, C. F. Kennel, W. S. Kurth, and D. A. Gurnett, Detection of Jovian whistler mode chorus: Implications for the Io torus aurora, *Geophys. Res. Lett., 7,* 45, 1980.

Coroniti, F. V., F.L. Scarf, C. F. Kennel,and W. S. Kurth, Analysis of chorus emissions at Jupiter, *J. Geophys. Res., 89,* 3801, 1984.

Eshleman, V. R., G. L. Tyler, J. D. Anderson, G. Fjeldbo, G. S. Levy, G. E. Wood, and T. A. Croft, Radio science investigations with Voyager, *Space Sci. Rev., 21,* 207, 1977.

Eshleman, V. R., G. L. Tyler, G. E. Wood, G. F. Lindal, J. D. Anderson, G. S. Levy, and T. A. Croft, Radio science with Voyager 1 at Jupiter: Preliminary profiles of the atmosphere and ionosphere, *Science, 204,* 976, 1979*a*.

Eshleman, V. R., G. L. Tyler, G. E. Wood, G. F. Lindal, J. D. Anderson, G. S. Levy, and T. A. Croft, Radio science with Voyager at Jupiter: Initial Voyager 2 results and a Voyager 1 measure of the Io torus, *Science, 206*, 959, 1979*b*.

Fillius, W., C. McIlwain, A. Mogro-Campero, and G. Steinberg, Evidence that pitch angle scattering is an important loss mechanism in the inner radiation belt of Jupiter, *Geophys. Res. Lett., 3*, 33, 1976.

Gurnett, D. A., F. L. Scarf, W. S. Kurth, R. R. Shaw, and R. L. Poynter, Determination of Jupiter's electron density profile from plasma wave observations, *J. Geophys. Res., 86*, 8199, 1981.

Hinson, D. P., Radio scintillations observed during atmospheric occultations of Voyager: Internal gravity waves at Titan and magnetic field orientations at Jupiter and Saturn, Ph.D thesis, Stanford Univ., Stanford, Ca., 1983.

Hinson, D. P., and G. L. Tyler, Spatial irregularities in Jupiter's upper ionosphere observed by Voyager radio occultations, *J. Geophys. Res., 87*, 5289, 1982.

Inan, U. S., T. F. Bell, and R. A. Helliwell, Nonlinear pitch angle scattering of energetic electrons by coherent VLF waves in the magnetosphere, *J. Geophys. Res., 83*, 3235, 1978.

Inan, U. S., T. F. Bell, and H. C. Chang, Particle precipitation induced by short-duration VLF waves in the magnetosphere, *J. Geophys. Res., 87*, 6243, 1982.

Inan, U. S., R. A. Helliwell, and W. S. Kurth, Terrestrial versus Jovian VLF chorus: a comparative study, *J. Geophys. Res., 88*, 6171, 1983.

Inan, U. S., H. C. Chang, R. A. Helliwell, W. L. Imhof, J. B. Reagan, and M. Walt, Precipitation of radiation belt electrons by man-made waves: A comparison between theory and measurements, *J. Geophys. Res., 90*, 359, 1985.

Krimigis, S. M., T. P. Armstrong, W. I. Axford, C. O. Bostrom, C. Y. Fan, G. Gloeckler, L. J. Lanzerotti, E. P. Keath, R. D. Zwickl, K. F. Carbary, and D. C. Hamilton, Low-energy charged particle environment at Jupiter: A first look, *Science, 204*, 998, 1979. 1981.

Lindal, G. T., G. E. Wood, G. S. Levy, J. D. Anderson, D. N. Sweetman, H. B. Hotz, B. J. Buckles, D. P. Holmes, P. E. Doms, V. R. Eshleman, G. L. Tyler, and T. A. Croft, The atmosphere of Jupiter: An analysis of the Voyager radio occultation measurements, *J. Geophys. Res., 86*, 8721, 1981.

Sandel, W. R., D. E. Shemansky, A. L. Broadfoot, J. L. Bertaux, J. E. Blamont, M. J. F. Belton, J. Ajello, J. B. Holberg, J. K. Atreya, T. M. Donahue, H. W. Moos, D. F. Strobel, J. C. McConnell, A. Dalgarno, R. Goody, M. B. McElroy, and R. Takacs, Extreme ultraviolet observations from Voyager 2 encounter with Jupiter, *Science, 206*, 962, 1979.

Scarf, F. L., D. A. Gurnett, and W. S. Kurth, Jupiter plasma wave observations: An initial Voyager 1 overview, *Science, 204*, 991, 1979*a*.

Scarf, F. L., F. V. Coroniti, D. A. Gurnett, and W. S. Kurth, Pitch-angle diffusion by whistler mode waves near the Io plasma torus, *Geophys. Res. Lett., 6*, 653, 1979*b*.

Scarf, F. L., D. A. Gurnett, and W. S. Kurth, Measurements of plasma wave spectra in Jupiter's magnetosphere, *J. Geophys. Res., 86*, 8181, 1981.

Scudder, J. D., E. C. Sittler, Jr., and H. S. Bridge, A survey of the plasma electron environment of Jupiter: A view from Voyager, *J. Geophys. Res., 86*, 8157, 1981.

Smith, A. J., D. L. Carpenter, and U. S. Inan, Whistler-triggered VLF noise bursts observed on the DE-1 satellite and simultaneously at Antarctic ground stations, *Ann. Geophys., 3*, 81, 1985.

Thorne, R. M., Microscopic plasma processes; in *Physics of the Jovian Magnetosphere*, edited by A. Dessler, p.00 Cambridge University Press, New York, 1983.

Waite, J. H., T. E. Cravens, J. Kozyra, A. F. Nagy, and S. K. Atreya, Electron precipitation and related aeronomy of the Jovian thermosphere and ionosphere, *J. Geophys. Res., 88*, 6143, 1983.

U. S. Inan, STAR Laboratory, Stanford University, Stanford, CA 94305.

(Received August 12, 1985;
revised November 4, 1985;
accepted November 13, 1985.)